Available at
www.ElsevierComputerScience.com
POWERED BY SCIENCE DIRECT

Computer Aided Geometric Design 20 (2003) 435–454

COMPUTER AIDED GEOMETRIC DESIGN

www.elsevier.com/locate/cagd

Rational approximation schemes for rotation-minimizing frames on Pythagorean-hodograph curves

Rida T. Farouki *, Chang Yong Han

Department of Mechanical and Aeronautical Engineering, University of California, Davis, CA 95616, USA

Received 4 February 2003; received in revised form 31 May 2003; accepted 1 June 2003

Abstract

An *adapted frame* $(\mathbf{t},\mathbf{u},\mathbf{v})$ on a space curve $\mathbf{r}(\xi)$ is a right-handed set of three orthonormal vectors, where $\mathbf{t}$ is the unit tangent and $\mathbf{u}$, $\mathbf{v}$ span the curve normal plane. For such frames to have a rational dependence on the curve parameter, $\mathbf{r}(\xi)$ must be a Pythagorean-hodograph (PH) curve, since only PH curves have rational unit tangent vectors. Among all possible adapted frames, the *rotation-minimizing frame* (RMF) is the most attractive for applications such as animation, swept surface constructions, and motion planning. The PH curves admit exact RMF descriptions, but they involve transcendental (logarithmic) functions. Since rational forms are generally preferred, the problem of rational approximation of RMFs for PH curves is considered herein. This is accomplished by employing the *Euler–Rodrigues frame* (ERF) as a reference (the ERF is rational and, unlike the Frenet frame, does not suffer indeterminacies at inflections). The function that describes the angular deviation between the RMF and ERF is derived in closed form, and is approximated by Padé (rational Hermite) interpolation. In typical cases, these interpolants furnish compact approximations of excellent accuracy, amenable to use in a variety of applications.

Keywords: Space curves; Rotation-minimizing frame; Euler–Rodrigues frame; Frenet frame; Pythagorean-hodograph curves; Quaternions; Energy integral; Padé approximation; Rational Hermite interpolation

1. Introduction

An *adapted frame* on a regular space curve $\mathbf{r}(\xi)$ is a right-handed orthonormal system of vector fields $\mathbf{t}(\xi)$, $\mathbf{u}(\xi)$, $\mathbf{v}(\xi)$, where $\mathbf{t}(\xi)=\mathbf{r}'(\xi)/|\mathbf{r}'(\xi)|$ is the unit tangent. There are many possible choices (Bishop, 1975) for $\mathbf{u}(\xi)$ and $\mathbf{v}(\xi)$, compatible with the requirement that $\mathbf{t}(\xi)=\mathbf{u}(\xi)\times\mathbf{v}(\xi)$—they can be derived from each other by rotations in the curve normal plane at each point.

* Corresponding author.
E-mail addresses: farouki@ucdavis.edu (R.T. Farouki), cyhan@ucdavis.edu (C.Y. Han).

0167-8396/$ – see front matter
doi:10.1016/S0167-8396(03)00095-5

The cumulative arc length function along the curve $\mathbf{r}(\xi)$ is defined by

$$s(\xi)=\int_0^{\xi}\left|\mathbf{r}'(t)\right|\mathrm{d}t.$$

Throughout this paper, primes indicate derivatives with respect to the curve parameter ξ, and dots denote derivatives with respect to the arc length s—such derivatives are related by

$$\frac{\mathrm{d}}{\mathrm{d}s}=\frac{1}{|\mathbf{r}'(\xi)|}\frac{\mathrm{d}}{\mathrm{d}\xi}.$$

Now the Cartesian components of the frame vectors yield the matrix

$$\mathbf{A}=[\,\mathbf{t}\quad\mathbf{u}\quad\mathbf{v}\,]=\begin{bmatrix} t_x & u_x & v_x \\ t_y & u_y & v_y \\ t_z & u_z & v_z \end{bmatrix},$$

and since $(\mathbf{t},\mathbf{u},\mathbf{v})$ form a basis in $\mathbb{R}^3$, the arc-length derivative of $\mathbf{A}$ must be expressible in the form

$$\dot{\mathbf{A}}=\mathbf{A}\,\mathbf{C}.$$

From the relations $|\mathbf{t}|=|\mathbf{u}|=|\mathbf{v}|=1$ and $\mathbf{t}\cdot\mathbf{u}=\mathbf{u}\cdot\mathbf{v}=\mathbf{v}\cdot\mathbf{t}=0$, one can easily see that the *Cartan connection matrix* has the skew-symmetric form

$$\mathbf{C}=\begin{bmatrix} 0 & -\gamma & \beta \\ \gamma & 0 & -\alpha \\ -\beta & \alpha & 0 \end{bmatrix},$$

where $\alpha=\dot{\mathbf{u}}\cdot\mathbf{v}$, $\beta=\dot{\mathbf{v}}\cdot\mathbf{t}$, $\gamma=\dot{\mathbf{t}}\cdot\mathbf{u}$. Equivalently, we may write

$$\frac{\mathrm{d}\mathbf{t}}{\mathrm{d}s}=\boldsymbol{\omega}\times\mathbf{t},\qquad \frac{\mathrm{d}\mathbf{u}}{\mathrm{d}s}=\boldsymbol{\omega}\times\mathbf{u},\qquad \frac{\mathrm{d}\mathbf{v}}{\mathrm{d}s}=\boldsymbol{\omega}\times\mathbf{v},\tag{1}$$

where the angular velocity vector $\boldsymbol{\omega}$ for the frame $(\mathbf{t},\mathbf{u},\mathbf{v})$ is defined by

$$\boldsymbol{\omega}=\alpha\mathbf{t}+\beta\mathbf{u}+\gamma\mathbf{v}.\tag{2}$$

The most familiar case of an adapted frame is the *Frenet frame*, for which $\mathbf{u}$ and $\mathbf{v}$ are the normal $\mathbf{n}$ and binormal $\mathbf{b}$, respectively, defined (Kreyszig, 1959; Struik, 1988) by

$$\mathbf{n}=\frac{\mathbf{r}'\times\mathbf{r}''}{|\mathbf{r}'\times\mathbf{r}''|}\times\mathbf{t},\qquad \mathbf{b}=\mathbf{t}\times\mathbf{n}.\tag{3}$$

For a polynomial or rational curve $\mathbf{r}(\xi)$, however, the frame $(\mathbf{t},\mathbf{n},\mathbf{b})$ does not depend rationally[1] on the curve parameter ξ. Also, $\mathbf{n}$ and $\mathbf{b}$ are undefined at *inflections*, where $\mathbf{r}''$ is parallel to $\mathbf{r}'$ or vanishes (in fact, they may experience sudden reversals through such points—see Fig. 5).

For the Frenet frame, we have $(\alpha,\beta,\gamma)=(\tau,0,\kappa)$ where

$$\kappa=\frac{|\mathbf{r}'\times\mathbf{r}''|}{|\mathbf{r}'|^3}\quad\text{and}\quad\tau=\frac{(\mathbf{r}'\times\mathbf{r}'')\cdot\mathbf{r}'''}{|\mathbf{r}'\times\mathbf{r}''|^2}\tag{4}$$

[1] A special class of curves that do possess rational Frenet frames is discussed in (Wagner and Ravani, 1997).

are the curvature and torsion. Correspondingly, the angular velocity (2) for the Frenet frame becomes the *Darboux vector*

$$\mathbf{d} = \kappa\mathbf{b} + \tau\mathbf{t}, \tag{5}$$

and $|\mathbf{d}| = \sqrt{\kappa^2 + \tau^2}$ is sometimes called the "total curvature" (Kreyszig, 1959; Struik, 1988).

Now for any adapted frame $(\mathbf{t}, \mathbf{u}, \mathbf{v})$ the component $\alpha\,\mathbf{t}$ of the angular velocity vector (2) corresponds to an instantaneous rotation of $\mathbf{u}$ and $\mathbf{v}$ in the normal plane of the curve. This component is not essential to the definition of an adapted frame—in fact, it is always possible to construct an adapted frame that lacks this "unnecessary" component. Such a frame, characterized by the property that $\alpha \equiv 0$, is called a *rotation-minimizing frame* (RMF). For an RMF, the angular velocity vector can be written as

$$\boldsymbol{\omega} = \beta\mathbf{u} + \gamma\mathbf{v} = -(\dot{\mathbf{t}} \cdot \mathbf{v})\mathbf{u} + (\dot{\mathbf{t}} \cdot \mathbf{u})\mathbf{v}, \tag{6}$$

where we note that $\dot{\mathbf{v}} \cdot \mathbf{t} = -\dot{\mathbf{t}} \cdot \mathbf{v}$, since $\mathbf{v} \cdot \mathbf{t} = 0$. Now $\dot{\mathbf{t}}$ lies in the normal plane spanned by $\mathbf{u}$ and $\mathbf{v}$ (since $|\mathbf{t}| = 1$), and we can write $\dot{\mathbf{t}} = \mu\mathbf{u} + \nu\mathbf{v}$. By substituting into (6), we find that $\boldsymbol{\omega} = -\nu\mathbf{u} + \mu\mathbf{v}$—i.e., for an RMF, $\boldsymbol{\omega}$ is just a rotation of $\dot{\mathbf{t}}$ by $\frac{1}{2}\pi$ in the normal plane. For the Frenet frame, on the other hand, the second basis vector $\mathbf{n}$ is chosen so as to always lie in the direction of $\dot{\mathbf{t}}$, and this choice means that $\alpha \not\equiv 0$.

The RMF finds important applications in animation and motion control, where the orientation of a rigid body must be specified as its center of mass executes a given spatial trajectory. Aligning the body's principal axes with the RMF at each point offers a natural solution to this problem, that avoids the "unnecessary" normal-plane rotation and inflectional indeterminacies[2] of the Frenet frame. Another application is in the construction of swept surfaces (Klok, 1986), defined by the motion of a "profile" curve along a "sweep" curve: using the RMF to orient the profile curve within the normal plane avoids undesired "twisting" of the swept surface. Finally, the RMF provides a solution to the problem of energy minimization for framed space curves (see Section 2 below).

Unfortunately, the polynomial and rational curves employed in computer graphics, computer-aided design, robotics, and similar applications do not admit simple closed-form descriptions for their RMFs. Consequently, several schemes have been proposed to approximate the rotation-minimizing frame of a given curve, or to approximate a given curve by "simpler" segments (e.g., circular arcs) with known rotation-minimizing frames (Jüttler, 1998; Jüttler and Mäurer, 1999a, 1999b; Wang and Joe, 1997).

An *exact* derivation of the RMF is possible (Farouki, 2002) for spatial *Pythagorean-hodograph* (PH) *curves* (Farouki et al., 2002a, 2002b)—but this involves the solution of quartic equations, and the use of transcendental (logarithmic) functions. PH curves incorporate algebraic structures that offer unique computational advantages. For example, only PH curves can have rational adapted frames—since only PH curves have rational unit tangent vectors. Furthermore, the arc lengths of PH curves can be computed *precisely*, and one can formulate real-time interpolators to drive multi-axis CNC machines along curved paths, at fixed or varying speeds, from their exact analytic descriptions (Farouki et al., 1998; Farouki and Shah, 1996; Tsai et al., 2001).

Since rational forms are preferred in computer graphics and computer-aided design applications, we consider here rational approximation schemes for RMFs on spatial PH curves. We employ the *Euler–Rodrigues frame* as a reference, which has distinct advantages over the Frenet frame. The ERF was introduced in (Choi and Han, 2002), and arises specifically from the quaternion representation of spatial PH curves in a particular Cartesian coordinate system. The angular deviation of the RMF, relative to the

[2] See Example 5 in Section 5 below.

ERF, is derived as a transcendental function, and Padé (rational Hermite) approximations to this function are constructed. For typical PH quintics, a rational rotation applied to the ERF offers a highly accurate approximation of the RMF.

This paper is organized as follows. In Section 2 we review the relation between RMFs and the problem of energy minimization for framed space curves. The function characterizing the angular deviation between the RMF and ERF is then derived in Section 3. In Section 4 we describe a scheme for the construction of Padé (i.e., rational Hermite) interpolants to this function, yielding rational RMF approximations. The performance of this scheme is illustrated through some computed examples in Section 5. Finally, in Section 6 we summarize our results and make some concluding remarks.

2. Deformation energy of elastic rods

In the theory of plane curves, the energy integral

$$E = \int_0^S \kappa^2 \, \mathrm{d}s \tag{7}$$

is used as a measure of "fairness" for a curve of total length S. This integral is proportional to the strain energy stored in a thin elastic beam, bent from an initially-straight configuration into the shape of the curve (Farouki, 1996). Minimization of E subject to interpolation constraints (and possibly also $S=$ constant) is a basic approach to the construction of "fair" curves.

Since curvature alone does not characterize the intrinsic geometry of non-planar curves, the question arises as to how the integral (7) can be generalized into an appropriate fairness measure for space curves. The theory of elastic spatial rods is much more subtle and involved (Dill, 1992; Landau and Lifshitz, 1986; Lembo, 2001; Love, 1944; Steigmann and Faulkner, 1993) than that of planar beams. A basic difference between the planar and spatial problems is that, for the latter, the "twist" of the elastic rod about its center line is an important contribution to the energy. This twist—which should not be confused with (and is quite independent of) the torsion function in (4)—is specified by superposing an adapted frame on the curve. Following (Landau and Lifshitz, 1986), we review below the energy integral appropriate to a "framed space curve," and highlight the significance of the RMF in this context.

Consider the deformation of a thin initially-straight elastic rod with total length S and circular cross section of radius $r \ll S$. The deformation includes both bending and twisting of the rod, but the total length S is unchanged. We define coordinates (ξ, ζ, η) in the deformed rod such that, in the undeformed state, they coincide with Cartesian coordinates (x, y, z) where the rod center line lies along the x-axis. After deformation, the orthonormal frame $(\mathbf{t}, \mathbf{u}, \mathbf{v})$ associated with the coordinates (ξ, ζ, η) rotates continuously along the length of the rod: $\mathbf{t}$ is the tangent to the center-line, while $\mathbf{u}$ and $\mathbf{v}$ span the cross-sectional plane. This rotation is specified by the angular velocity vector

$$\boldsymbol{\omega} = \frac{\mathrm{d}\boldsymbol{\phi}}{\mathrm{d}s},$$

where $\mathrm{d}\boldsymbol{\phi}$ is the (vector) infinitesimal frame rotation associated with an arc length increment $\mathrm{d}s$, through the relations (1). Now if we express the angular velocity vector $\boldsymbol{\omega}$ in terms of components as

$\omega_\xi \mathbf{t} + \omega_\zeta \mathbf{u} + \omega_\eta \mathbf{v}$, the work done in deforming the rod from the initial straight configuration—i.e., the elastic strain energy stored in the deformed rod—can be written (Landau and Lifshitz, 1986) as

$$U = \int_0^S \tfrac{1}{2} G J \omega_\xi^2 + \tfrac{1}{2} E I \left(\omega_\zeta^2 + \omega_\eta^2\right) \mathrm{d}s.$$

E and G are the Young's modulus and shear modulus (modulus of rigidity) of the material and, for a circular cross section of radius r, the quantities

$$I = \frac{\pi r^4}{4} \quad \text{and} \quad J = \frac{\pi r^4}{2}$$

are the second moment of area about a diameter, and second polar moment of area about the center. The term $\frac{1}{2} E I(\omega_\zeta^2 + \omega_\eta^2)$ in the integrand represents the bending energy per unit length, while $\frac{1}{2} G J \omega_\xi^2$ is the twisting energy per unit length. Introducing the material constitutive relation

$$G = \frac{E}{2(1+\nu)},$$

where ν is Poisson's ratio, the energy integral may be expressed as

$$U = \frac{\pi r^4 E}{8} \int_0^S k\omega_\xi^2 + \omega_\zeta^2 + \omega_\eta^2 \, \mathrm{d}s, \tag{8}$$

where $k = 1/(1+\nu)$. For most metals $\nu \approx 0.3$, and hence $k \approx 0.75$ can be used as a "canonical" value for this weighting factor.

It is evident that we cannot speak of the energy of a space curve without also specifying an adapted frame along the curve: the adapted frame serves to fix the amount of "twisting" of the elastic rod about its center-line axis,[3] which is an additional source of strain energy. Comparing with (2), we see that $\alpha = \omega_\xi$, $\beta = \omega_\zeta$, $\gamma = \omega_\eta$. Thus, if the twist of the elastic rod is defined by the Frenet frame, the integrand in (8) becomes $k\tau^2 + \kappa^2$, and the twist of the rod evidently makes a non-zero contribution in this case.

Now taking cross products of the first equation in (1) with $\mathbf{t}$ gives

$$\boldsymbol{\omega} = (\mathbf{t} \cdot \boldsymbol{\omega})\mathbf{t} + \mathbf{t} \times \frac{\mathrm{d}\mathbf{t}}{\mathrm{d}s},$$

and since $\mathbf{t} \cdot \boldsymbol{\omega} = \omega_\xi$ and $\mathrm{d}\mathbf{t}/\mathrm{d}s = \kappa \mathbf{n}$, where κ is the curvature and $\mathbf{n}$ is the normal vector, we obtain

$$\boldsymbol{\omega} = \omega_\xi \mathbf{t} + \kappa \mathbf{b},$$

where $\mathbf{b} = \mathbf{t} \times \mathbf{n}$ is the binormal vector. Thus, for *any* choice of $\mathbf{u}$ and $\mathbf{v}$ we always have $\omega_\zeta \mathbf{u} + \omega_\eta \mathbf{v} = \kappa \mathbf{b}$, and hence

$$\omega_\zeta^2 + \omega_\eta^2 = \kappa^2 = \left| \frac{\mathrm{d}\mathbf{t}}{\mathrm{d}s} \right|^2.$$

Hence, the integrand in (8) always has the form $k\omega_\xi^2 + \kappa^2$, and for a given curve its smallest value at each point is realized when $\omega_\xi \equiv 0$—i.e., the adapted frame chosen to specify the "twist" is an RMF.

[3] This twisting is independent (Love, 1944) of the torsion τ in (4). Whereas the latter is fixed by the intrinsic geometry, the twist ω_ξ can be arbitrarily imposed on a given space curve.

Since choosing an RMF gives the least possible value for the integral (8), among all possible adapted frames, it is natural to use this choice in defining an "intrinsic" energy for space curves—that depends only on their shapes, and is independent of the manner in which they are framed. Since $\omega_\xi \equiv 0$ for an RMF, and $\omega_\zeta^2 + \omega_\eta^2 = \kappa^2$ for any adapted frame, with this choice the energy integral (8) for space curves clearly coincides—up to a multiplicative constant—with the energy integral (7) for planar curves.

3. RMF and ERF on PH curves

Since polynomial and rational curves do not, in general, admit rational RMF representations, approximations are necessary to conform to the prevailing representation schemes in computer-aided geometric design. For any adapted frame, exactitude of the curve tangent field $\mathbf{t}(\xi)$ is one attribute that should not be compromised by the approximation scheme. Since only the PH curves admit rational unit tangents, our focus henceforth will be on rational RMF approximations for spatial PH curves using the quaternion representation (Choi et al., 2002).

Given a quaternion polynomial

$$\mathcal{A}(\xi) = u(\xi) + v(\xi)\mathbf{i} + p(\xi)\mathbf{j} + q(\xi)\mathbf{k} \tag{9}$$

of degree d, integration of the hodograph

$$\mathbf{r}'(\xi) = \mathcal{A}(\xi)\mathbf{i}\mathcal{A}^*(\xi), \tag{10}$$

where $\mathcal{A}^*(\xi) = u(\xi) - v(\xi)\mathbf{i} - p(\xi)\mathbf{j} - q(\xi)\mathbf{k}$, defines a PH curve $\mathbf{r}(\xi)$ of degree $2d+1$. The hodograph components satisfy the Pythagorean condition

$$x'^2(\xi) + y'^2(\xi) + z'^2(\xi) \equiv \sigma^2(\xi), \tag{11}$$

where

$$\begin{aligned}
x'(\xi) &= u^2(\xi) + v^2(\xi) - p^2(\xi) - q^2(\xi),\\
y'(\xi) &= 2\big[u(\xi)q(\xi) + v(\xi)p(\xi)\big],\\
z'(\xi) &= 2\big[v(\xi)q(\xi) - u(\xi)p(\xi)\big],\\
\sigma(\xi) &= u^2(\xi) + v^2(\xi) + p^2(\xi) + q^2(\xi).
\end{aligned} \tag{12}$$

The above form is sufficient and necessary (Dietz et al., 1993) to satisfy (11), and is invariant (Farouki et al., 2002a) under general spatial rotations. The quaternion representation (10) for the form (12), and its resulting rotation invariance, have also been noted by Wallner and Pottmann (1997), in the context of blending surface constructions for quadrics. Additional details on the construction and properties of spatial PH curves in the quaternion representation may be found in (Farouki et al., 2002a, 2002b, 2003).

Corresponding to the hodograph (10), an adapted rational frame on $\mathbf{r}(\xi)$—the so-called Euler–Rodrigues frame (ERF)—is defined (Choi and Han, 2002) by

$$\mathbf{t}(\xi) = \frac{\mathcal{A}(\xi)\mathbf{i}\mathcal{A}^*(\xi)}{\mathcal{A}(\xi)\mathcal{A}^*(\xi)}, \qquad \mathbf{u}(\xi) = \frac{\mathcal{A}(\xi)\mathbf{j}\mathcal{A}^*(\xi)}{\mathcal{A}(\xi)\mathcal{A}^*(\xi)}, \qquad \mathbf{v}(\xi) = \frac{\mathcal{A}(\xi)\mathbf{k}\mathcal{A}^*(\xi)}{\mathcal{A}(\xi)\mathcal{A}^*(\xi)}. \tag{13}$$

Unlike the Frenet frame, the ERF is defined at every point of a PH curve. Moreover, if $\mathbf{r}(\xi)$ is of degree $2d+1$, the ERF has a rational dependence of degree $2d$ on the curve parameter. For a given a PH curve, the ERF is not uniquely defined, since the quaternion representation of the PH curve is not unique (Farouki et al., 2002a). However, this ambiguity is not essential, since each pair of ERFs maintain a constant angular difference along the curve.

Now the quantities $(\alpha, \beta, \gamma) = (\omega_\xi, \omega_\zeta, \omega_\eta)$ introduced in Sections 1 and 2 were defined in terms of arc-length derivatives. It is more convenient, henceforth, to define them in terms of parametric derivatives. For a PH curve, the two definitions differ only by a factor of σ, the *parametric speed* of the curve. For the PH curve specified by (10), we then have (Choi and Han, 2002):

$$\alpha = \mathbf{u}' \cdot \mathbf{v} = 2\frac{uv' - u'v - pq' + p'q}{u^2 + v^2 + p^2 + q^2}.$$

A non-trivial PH curve having $\alpha \equiv 0$ (i.e., the ERF and RMF are coincident) must be (Choi and Han, 2002) of degree $\geqslant 7$. Since no algorithms are currently available that allow this class of curves to be used in practical design problems, we focus on the PH quintics—for which such algorithms are known (Farouki et al., 2002b, 2003)—and seek rational rotations of the ERF about $\mathbf{t}$ that closely approximate an RMF.

Let $(\tilde{\mathbf{t}}, \tilde{\mathbf{u}}, \tilde{\mathbf{v}})$ be a rotation of the ERF about the tangent, such that

$$\tilde{\mathbf{t}}(\xi) = \mathbf{t}(\xi), \qquad \begin{bmatrix} \tilde{\mathbf{u}}(\xi) \\ \tilde{\mathbf{v}}(\xi) \end{bmatrix} = \begin{bmatrix} \cos\theta(\xi) & \sin\theta(\xi) \\ -\sin\theta(\xi) & \cos\theta(\xi) \end{bmatrix} \begin{bmatrix} \mathbf{u}(\xi) \\ \mathbf{v}(\xi) \end{bmatrix}.$$

Then, as expected, we have

$$\tilde{\alpha} = \tilde{\mathbf{u}}' \cdot \tilde{\mathbf{v}} = \theta' + \alpha,$$

i.e., the angular speed (about $\mathbf{t}$) of the rotated frame is its angular speed with respect to the reference frame, plus the angular speed of the reference frame itself. Hence, the rotated frame coincides with the RMF if and only if $\theta(\xi)$ satisfies[4]

$$\theta' = -\alpha = 2\frac{u'v - uv' - p'q + pq'}{u^2 + v^2 + p^2 + q^2}. \tag{14}$$

An exact computation of $\theta(\xi)$ requires the integration of a rational function of degree $2d$. In general, this integration incurs transcendental (logarithmic) functions in $\theta(\xi)$, so we cannot expect $\cos\theta(\xi)$ and $\sin\theta(\xi)$, and the RMF, to be rational. For details of this exact integration—using the Frenet frame, rather than the ERF, as a reference[5]—see (Farouki, 2002).

Instead of exact integration, we employ rational approximation. Let $\phi(\xi)$ be an approximation of $\theta(\xi)$, such that

$$\sin\phi(\xi) = \frac{a^2(\xi) - b^2(\xi)}{a^2(\xi) + b^2(\xi)}, \qquad \cos\phi(\xi) = \frac{2a(\xi)b(\xi)}{a^2(\xi) + b^2(\xi)}$$

[4] Since the RMF is characterized by a differential constraint, there is a one-parameter family of RMFs, corresponding to the choice of an initial orientation on integrating (14).

[5] The angular difference between the RMF and the Frenet frame is simply the integral of the torsion with respect to arc length (Farouki, 2002; Guggenheimer, 1989).

for some polynomials $a(\xi)$ and $b(\xi)$. In other words, we are trying to construct a rational parameterization of the circle,[6] such that the corresponding angular variation $\phi(\xi)$ closely approximates the known (transcendental) function $\theta(\xi)$. One can easily verify that

$$\tfrac{1}{2}\phi' = \frac{a'b - ab'}{a^2 + b^2} = \frac{\mathrm{d}}{\mathrm{d}\xi} \arctan \frac{a}{b},$$

and hence ϕ is a good approximation of θ if and only if a/b is a good rational approximation of the function

$$f(\xi) = \tan \tfrac{1}{2}\theta(\xi) = \tan \int \frac{g(\xi)}{h(\xi)}\,\mathrm{d}\xi, \tag{15}$$

where

$$g(\xi) = u'(\xi)v(\xi) - u(\xi)v'(\xi) - p'(\xi)q(\xi) + p(\xi)q'(\xi), \tag{16}$$

and

$$h(\xi) = u^2(\xi) + v^2(\xi) + p^2(\xi) + q^2(\xi). \tag{17}$$

As a measure of the quality of approximation, we compare the exact function $\theta(\xi) = 2\int g(\xi)/h(\xi)\,\mathrm{d}\xi$ with the approximation $\phi(\xi) = 2\arctan a(\xi)/b(\xi)$.

4. Rational Hermite interpolation scheme

The possibility of rational adapted frames on space curves was first observed in the early study (Farouki and Sakkalis, 1994) of spatial PH curves, which employed a representation that is sufficient (but not necessary) for a Pythagorean hodograph. Jüttler and Mäurer (1999b) subsequently described RMF approximations for PH cubics. Since PH cubics have rather limited shape flexibility, we focus here on general rational RMF approximations for quintic or higher-order PH curves.

To approximate (15) by a rational function $a(\xi)/b(\xi)$, we use multi-point Padé approximation, which is equivalent to rational Hermite interpolation. For background on this topic, the reader may consult (Baker and Graves-Morris, 1996; Brezinski and Van Iseghem, 1994; Cuyt, 1992).

Consider a function $f(\xi)$ and a set of distinct points $\xi_0, \ldots, \xi_r \in [0, 1]$ where, at each point ξ_i, the function value and derivatives $f^{(k)}(\xi_i)$ are given for $k = 0, \ldots, s_i - 1$ ($s_i > 0$). The rational Hermite interpolation problem of order (m, n) for $f(\xi)$ amounts to the construction of polynomials

$$a(\xi) = \sum_{i=0}^{m} a_i \xi^i \quad \text{and} \quad b(\xi) = \sum_{i=0}^{n} b_i \xi^i,$$

such that

$$\sum_{i=0}^{r} s_i = m + n + 1 \tag{18}$$

[6] Rational parameterizations of circles are discussed extensively in the literature (Bangert and Prautzsch, 1997; Chou, 1995; Fiorot et al., 1997; Piegl and Tiller, 1989). The goal in these studies is typically to achieve nearly-uniform parameterizations, while our present goal is to obtain rational approximations of a *specific* parameterization.

and

$$f^{(k)}(\xi_i) = \left(\frac{a}{b}\right)^{(k)}(\xi_i) \quad \text{for } k = 0, \ldots, s_i - 1;\ i = 0, \ldots, r. \tag{19}$$

Note that the sum of degrees of a and b is minimal to satisfy the interpolation conditions. Instead of directly using (19), we consider the conditions

$$(fb - a)^{(k)}(\xi_i) = 0 \quad \text{for } k = 0, \ldots, s_i - 1;\ i = 0, \ldots, r. \tag{20}$$

These conditions define a homogeneous system of $m + n + 1$ linear equations in the $m + n + 2$ unknown coefficients a_i and b_i of $a(\xi)$ and $b(\xi)$, and hence they always admit at least one non-trivial solution. In fact, if $a_1(\xi)$, $b_1(\xi)$ and $a_2(\xi)$, $b_2(\xi)$ both satisfy (20), then $a_1(\xi)b_2(\xi) \equiv a_2(\xi)b_1(\xi)$—i.e., all rational solutions of (20) have the same irreducible form.

Having computed a rational interpolant a/b from the linear interpolation conditions (i.e., the conditions expressed in terms of $fb - a$ instead of $f - a/b$), it may happen in certain exceptional cases that an interpolation point is also a common zero of a and b. At such points, the irreducible form of a/b may not interpolate the correct value. This problem may be remedied by checking for coincidence of the roots of $\gcd(a, b)$ with any of the nodes $\xi_0, \ldots, \xi_r$. When such coincidences occur, a higher order (m, n) for the rational interpolant is needed to achieve the prescribed interpolation conditions.

Now let $x_0, \ldots, x_{m+n}$ be a list of the distinct interpolation nodes $\xi_0, \ldots, \xi_r$ with each node repeated according to its multiplicity, i.e.,

$$\underbrace{x_0, \ldots, x_{s_0-1}}_{=\xi_0}, \underbrace{x_{s_0}, \ldots, x_{s_0+s_1-1}}_{=\xi_1}, \ldots, \underbrace{x_{s_0+\cdots+s_{r-1}}, \ldots, x_{s_0+\cdots+s_{r-1}+s_r-1}}_{=\xi_r}.$$

Then, for the given set of nodes and multiplicities, the divided differences of $f(\xi)$ are defined (Stoer and Bulirsch, 1992) recursively by

$$f[x_i] = f(x_i),$$

and

$$f[x_i, \ldots, x_{i+k}] = \begin{cases} \dfrac{f^{(k)}(x_i)}{k!} & \text{if } x_i = \cdots = x_{i+k}, \\[2ex] \dfrac{f[x_{i+1}, \ldots, x_{i+k}] - f[x_i, \ldots, x_{i+k-1}]}{x_{i+k} - x_i} & \text{otherwise.} \end{cases}$$

It is convenient to introduce the more compact notation

$$c_{i,j} = \begin{cases} 0 & i > j, \\ f[x_i, \ldots, x_j] & i \leqslant j. \end{cases}$$

If we then set

$$B_j(\xi) = \begin{cases} 1 & j = 0, \\ \displaystyle\prod_{k=1}^{j} (\xi - x_{k-1}) & \text{otherwise,} \end{cases}$$

and

$$F_{i,j}(\xi)=\begin{cases}0 & i>j,\\ \displaystyle\sum_{k=i}^{j} c_{i,k}B_k(\xi) & i\leqslant j,\end{cases}$$

the numerator and denominator of the rational interpolant $a(\xi)/b(\xi)$ can be formulated (Cuyt, 1992) as the determinants

$$a(\xi)=\begin{vmatrix} F_{0,m}(\xi) & F_{1,m}(\xi) & \cdots & F_{n,m}(\xi)\\ c_{0,m+1} & c_{1,m+1} & \cdots & c_{n,m+1}\\ c_{0,m+2} & c_{1,m+2} & \cdots & c_{n,m+2}\\ \cdots & \cdots & \cdots & \cdots\\ c_{0,m+n} & c_{1,m+n} & \cdots & c_{n,m+n}\end{vmatrix},$$

and

$$b(\xi)=\begin{vmatrix} B_0(\xi) & B_1(\xi) & \cdots & B_n(\xi)\\ c_{0,m+1} & c_{1,m+1} & \cdots & c_{n,m+1}\\ c_{0,m+2} & c_{1,m+2} & \cdots & c_{n,m+2}\\ \cdots & \cdots & \cdots & \cdots\\ c_{0,m+n} & c_{1,m+n} & \cdots & c_{n,m+n}\end{vmatrix}.$$

An explicit expansion of the determinants is not necessarily a good approach to computing $a(\xi)$ and $b(\xi)$, especially for large m and n. However, we are primarily interested in the low-degree case $m=n=2$, for which we obtain the simple closed-form expressions

$$\begin{aligned}a(\xi)={}&c_{0,0}[c_{1,4}c_{2,3}-c_{1,3}c_{2,4}]\\&+[c_{0,1}c_{1,4}c_{2,3}+c_{0,3}c_{1,1}c_{2,4}-c_{0,4}c_{1,1}c_{2,3}-c_{0,1}c_{1,3}c_{2,4}](\xi-x_0)\\&+[c_{0,2}c_{1,4}c_{2,3}+c_{0,3}c_{1,2}c_{2,4}+c_{0,4}c_{1,3}c_{2,2}\\&-c_{0,3}c_{1,4}c_{2,2}-c_{0,4}c_{1,2}c_{2,3}-c_{0,2}c_{1,3}c_{2,4}](\xi-x_0)(\xi-x_1)\end{aligned}\tag{21}$$

and

$$\begin{aligned}b(\xi)={}&c_{1,4}c_{2,3}-c_{1,3}c_{2,4}+[c_{0,3}c_{2,4}-c_{0,4}c_{2,3}](\xi-x_0)\\&+[c_{0,4}c_{1,3}-c_{0,3}c_{1,4}](\xi-x_0)(\xi-x_1).\end{aligned}\tag{22}$$

To compute interpolant values and derivatives for the function (15) that we wish to approximate, we begin by noting that since the denominator of the integrand in (15) is quartic, it can be factorized by using Ferrari's method (Uspensky, 1948) to compute its roots z_1, z_2, z_3, z_4. In general, these roots are distinct, and we can use a partial fraction expansion to write the integrand as

$$\frac{g(\xi)}{h(\xi)}=\sum_{k=1}^{4}\frac{c_k}{\xi-z_k},$$

the coefficients (residues) c_k being found by clearing the denominators, and setting ξ equal to each root in succession, to obtain

$$c_k = \frac{g(z_k)}{\prod_{j\neq k}(z_k - z_j)}, \quad k = 1, \ldots, 4.$$

Integration then gives

$$\int \frac{g(\xi)}{h(\xi)}\,\mathrm{d}\xi = \theta_0 + \sum_{k=1}^{4} c_k \ln(\xi - z_k),$$

where θ_0 is an integration constant. Assuming that $\gcd(u, v, p, q) =$ constant, the roots of h must occur as complex conjugate pairs, and the corresponding residues are also complex conjugates. Logarithmic terms that correspond to such pairs can be combined to give explicitly real expressions—for example, if $z, \bar{z}$ and $c, \bar{c}$ are conjugate roots and residues, we have

$$c \ln(\xi - z) + \bar{c} \ln(\xi - \bar{z}) = 2\big[\mathrm{Re}(c) \ln|\xi - z| - \mathrm{Im}(c) \arg(\xi - z)\big].$$

Denoting the other pair of roots and corresponding residues by $w, \bar{w}$ and $d, \bar{d}$ so that

$$\frac{g(\xi)}{h(\xi)} = \frac{c}{\xi - z} + \frac{\bar{c}}{\xi - \bar{z}} + \frac{d}{\xi - w} + \frac{\bar{d}}{\xi - \bar{w}}, \tag{23}$$

we have

$$\int \frac{g(\xi)}{h(\xi)}\,\mathrm{d}\xi = 2\big[\mathrm{Re}(c) \ln|\xi - z| + \mathrm{Re}(d) \ln|\xi - w| \\ - \mathrm{Im}(c) \arg(\xi - z) - \mathrm{Im}(d) \arg(\xi - w)\big] + \theta_0. \tag{24}$$

Since this integral is subject to evaluation by the tangent function, one must be careful to choose the integration constant θ_0 such that the integral does not cross $(n + \frac{1}{2})\pi$ in the interval $\xi \in [0, 1]$ of interest. This can be done by evaluating the extrema of the integral, which are located at the real roots of $g(\xi)$ on $\xi \in (0, 1)$ or at the interval endpoints $\xi = 0$ and $\xi = 1$. In case the range of values of the integral is not contained within an interval of the form $(n - \frac{1}{2})\pi < \xi < (n + \frac{1}{2})\pi$, a further subdivision of $\xi \in [0, 1]$ is necessary.

Example 1. Consider the general PH quintic defined by

$$\begin{aligned} u(\xi) &= 4.86877 + 4.78126\xi + 3.32330\xi^2, \\ v(\xi) &= -6.43321 + 5.52435\xi + 2.85747\xi^2, \\ p(\xi) &= 2.83170 - 9.98047\xi - 7.28976\xi^2, \\ q(\xi) &= -1.53492 - 2.73598\xi + 9.65593\xi^2. \end{aligned}$$

Forming the polynomials (16) and (17), we have

$$\begin{aligned} &z, \bar{z} = -0.830350 \pm 0.828652\mathrm{i} \quad \text{and} \quad c, \bar{c} = 0.0125113 \pm 0.219377\mathrm{i}, \\ &w, \bar{w} = 0.359226 \pm 0.449591\mathrm{i} \quad \text{and} \quad d, \bar{d} = -0.0125113 \pm 0.312214\mathrm{i} \end{aligned}$$

in the partial fraction decomposition (23). The numerator $g(\xi)$ does not have real roots, and the right–hand side of (24) has the values $0.561425\pi + \theta_0$ at $\xi = 0$ and $0.188488\pi + \theta_0$ at $\xi = 1$. Hence, by setting $\theta_0 = -0.374956\pi$, the integral remains in the range $\pm 0.186469\pi$.

As evident from the above example, further structure can be discerned in the partial fraction decomposition (23) for general PH quintics.

Lemma 1. *For general PH quintics, the residues c and d in expression* (24) *satisfy* $\mathrm{Re}(c) + \mathrm{Re}(d) = 0$.

Proof. For general PH quintics, we have $\deg(g) = 2$ and $\deg(h) = 4$. Setting $h(\xi) = k(\xi - z)(\xi - \bar{z})(\xi - w)(\xi - \bar{w})$ and clearing denominators in (23) gives

$$g(\xi) = k(c + \bar{c} + d + \bar{d})\xi^3 + \text{lower order terms.}$$

Since $g(\xi)$ is just quadratic, we must have $c + \bar{c} + d + \bar{d} = 2\,\mathrm{Re}(c + d) = 0$, and hence $\mathrm{Re}(c) + \mathrm{Re}(d) = 0$. □

Hence, expression (24) can be simplified somewhat to yield

$$\int \frac{g(\xi)}{h(\xi)}\,\mathrm{d}\xi = 2\left[\mathrm{Re}(c)\ln\left|\frac{\xi - z}{\xi - w}\right| - \mathrm{Im}(c)\arg(\xi - z) - \mathrm{Im}(d)\arg(\xi - w)\right] + \theta_0.$$

We now consider RMF approximations for *helical* PH quintics (Farouki et al., 2003), which are characterized by the property that their tangents make a constant angle relative to a fixed line (the axis of the helix) in space. If a polynomial curve is helical, it must be a PH curve (Farouki et al., 2003). A sufficient condition (Farouki et al., 2003) for a general PH quintic to be helical is that the quadratic polynomial

$$\mathcal{A}(\xi) = \mathcal{A}_0(1 - \xi)^2 + \mathcal{A}_1 2(1 - \xi)\xi + \mathcal{A}_2\xi^2$$

employed in (10) has linearly-dependent quaternion coefficients $\mathcal{A}_0, \mathcal{A}_1, \mathcal{A}_2$.

Example 2. To define a helical PH quintic, we choose

$$\mathcal{A}_0 = 1.09868\mathbf{i} + 0.455090\mathbf{k},$$
$$\mathcal{A}_2 = -0.774033 + 0.328603\mathbf{i} + 0.779681\mathbf{j} - 0.314967\mathbf{k},$$
$$\mathcal{A}_1 = -2.60038(\mathcal{A}_0 + \mathcal{A}_2).$$

This corresponds to the “good” helical PH quintic interpolant to the Hermite data $\mathbf{r}(0) = (0, 0, 0)$, $\mathbf{r}'(0) = (1, 0, 1)$ and $\mathbf{r}(1) = (1, 1, 1)$, $\mathbf{r}'(1) = (0, 1, 1)$—see Example 4 in (Farouki et al., 2003). In the partial fraction expansion (23) we then have

$$z, \bar{z} = -0.234351 \pm 0.356555\mathrm{i} \quad \text{and} \quad c, \bar{c} = \pm 0.431258\mathrm{i},$$
$$w, \bar{w} = 1.23435 \pm 0.356555\mathrm{i} \quad \text{and} \quad d, \bar{d} = \pm 0.431258\mathrm{i}.$$

In this example, the structure of the roots $z, \bar{z}$ and $w, \bar{w}$ is a consequence of the symmetry of the Hermite data that define the curve. However, the fact that the residues c and d are pure imaginary numbers, of the same magnitude, is a generic property of helical PH quintics:

Lemma 2. *For general helical PH quintics, we have* $\mathrm{Re}(c) = \mathrm{Re}(d) = 0$ *and* $|\mathrm{Im}(c)| = |\mathrm{Im}(d)|$.

Proof. Any polynomial helix is necessarily a PH curve (Farouki et al., 2003), and without loss of generality we may choose the helical axis in the positive x-direction. The components of (9) then satisfy

$$u^2 + v^2 - p^2 - q^2 = \cos\psi\big(u^2 + v^2 + p^2 + q^2\big),$$

where ψ is the constant angle that the tangent makes with the axis. We can re-arrange the above equation to yield

$$(p - tu)(p + tu) = (tv - q)(tv + q)$$

or

$$(p - tv)(p + tv) = (tu - q)(tu + q),$$

where $t = \tan\frac{1}{2}\psi$. For a general PH quintic helix (i.e., with a doubly-traced tangent indicatrix), the above equations generate four pairs of solutions:

$$(p, q) = \pm t(u, v) \quad \text{or} \quad (p, q) = \pm t(-v, u). \tag{25}$$

Now since the function $g/h = -\frac{1}{2}\alpha$ is invariant under spatial rotations, we can rotate the curve such that the helical axis is aligned with the positive x-axis. Then conditions (25) hold, and we have

$$\frac{g}{h} = \frac{1 - t^2}{1 + t^2}\frac{u'v - uv'}{u^2 + v^2} = \cos\psi\frac{\mathrm{d}}{\mathrm{d}\xi}\arctan\frac{u}{v}.$$

As in (23), we can write

$$\frac{c}{\xi - z} + \frac{\bar{c}}{\xi - \bar{z}} + \frac{d}{\xi - w} + \frac{\bar{d}}{\xi - \bar{w}} = \frac{g(\xi)}{h(\xi)} = \cos\psi\frac{\mathrm{d}}{\mathrm{d}\xi}\arctan\frac{u(\xi)}{v(\xi)},$$

and by the Residue Theorem, we have

$$c = \frac{1}{2\pi\mathrm{i}}\oint_\gamma \frac{g}{h}\,\mathrm{d}\xi = \frac{\cos\psi}{2\pi\mathrm{i}}\oint_\gamma \frac{\mathrm{d}}{\mathrm{d}\xi}\arctan\frac{u}{v}\,\mathrm{d}\xi$$

for a sufficiently small closed curve γ enclosing the point z (γ is parameterized on the interval $[0, 1]$ and has winding number 1 with respect to z).

Now since $z, \bar{z}$ and $w, \bar{w}$ are roots of h, we have

$$\frac{u^2}{v^2} = -1$$

at those points, and we may assume that

$$\frac{u(z)}{v(z)} = \frac{u(w)}{v(w)} = \mathrm{i} \quad \text{and} \quad \frac{u(\bar{z})}{v(\bar{z})} = \frac{u(\bar{w})}{v(\bar{w})} = -\mathrm{i}.$$

The arctangent function has poles at $\pm\mathrm{i}$, and branch cuts from $+\mathrm{i}$ to $+\mathrm{i}\infty$ and from $-\mathrm{i}$ to $-\mathrm{i}\infty$. To apply the fundamental theorem of calculus

$$\oint_\gamma \frac{\mathrm{d}}{\mathrm{d}\xi}\arctan\frac{u}{v}\,\mathrm{d}\xi = \arctan\frac{u(\gamma(1))}{v(\gamma(1))} - \arctan\frac{u(\gamma(0))}{v(\gamma(0))}, \tag{26}$$

the image of γ under the map u/v should not cross the branch cuts—i.e., we should choose the start and end points of γ such that u/v at those points lies on the branch cut from $+\mathrm{i}$ to $+\mathrm{i}\infty$. Then the images of $u(\gamma(1))/v(\gamma(1))$ and $u(\gamma(0))/v(\gamma(0))$ under the arctangent function are, respectively, on the lines $\mathrm{Re}(\xi) = +\frac{1}{2}\pi$ and $\mathrm{Re}(\xi) = -\frac{1}{2}\pi$ with the same height. Hence, the value of the integral (26) is π, and we obtain $c = -\frac{1}{2}\cos\psi\mathrm{i}$. Identical arguments for the pole w yield $d = -\frac{1}{2}\cos\psi\mathrm{i}$. □

The above observation leads to the following interpretation for helical PH quintics. The quantity

$$\int \frac{g(\xi)}{h(\xi)}\,\mathrm{d}\xi = -2\,\mathrm{Im}(c)\big[\arg(\xi - z) \pm \arg(\xi - w)\big] + \theta_0$$

is just half the angular difference between the ERF and the RMF. As ξ traverses the real line from 0 to 1, the scaled sum (or difference) of the angular position of z and w (the two independent complex roots of h) relative to ξ is just this angular difference.

Lemma 1 is a special case of the "sum of residues rule" for real rational functions with numerator of degree two or more less than the degree of the denominator. For such rational functions, the residues always sum to zero. Lemma 2 is not so obvious—we are not aware of any simple geometrical interpretation or consequence of this lemma.

Once the rational approximation $a(\xi)/b(\xi)$ to (15) has been computed, we can use the approximation $\phi(\xi) = 2\arctan a(\xi)/b(\xi)$ to the angular deviation of the RMF from the ERF to construct the rational approximation

$$\begin{bmatrix} \hat{\mathbf{u}} \\ \hat{\mathbf{v}} \end{bmatrix} = \frac{1}{a^2 + b^2}\begin{bmatrix} b^2 - a^2 & 2ab \\ -2ab & b^2 - a^2 \end{bmatrix}\begin{bmatrix} \mathbf{u} \\ \mathbf{v} \end{bmatrix}$$

of the RMF, the ERF components $(\mathbf{u}, \mathbf{v})$ being given by (13). Since a, b are polynomials in ξ, and $(\mathbf{u}, \mathbf{v})$ depend rationally on ξ, it is clear that $(\hat{\mathbf{u}}, \hat{\mathbf{v}})$ have a rational dependence on ξ.

5. Computed examples

To interpolate C^1 Hermite data at $\xi = 0$ and 1 (four conditions), we must choose $a(\xi)$ linear and $b(\xi)$ quadratic, or vice-versa. Instead, we take both $a(\xi)$ and $b(\xi)$ quadratic, with an additional condition: interpolation at the midpoint, $\xi = \frac{1}{2}$. For the rational Hermite interpolation, we then have

$$\xi_0 = 0, \qquad \xi_1 = \tfrac{1}{2}, \qquad \xi_2 = 1,$$

$$x_0 = x_1 = 0, \qquad x_2 = \tfrac{1}{2}, \qquad x_3 = x_4 = 1,$$

and input data

$$f(0), \qquad f'(0), \qquad f\big(\tfrac{1}{2}\big), \qquad f(1), \qquad f'(1).$$

Note that $f^{(k)}(\xi_*)$ can be computed *exactly* for any ξ_* and $k = 0, 1, \ldots$. Eqs. (21) and (22) can then be written as follows:

$$a(\xi) = c_{0,0}A + (c_{0,1}A + c_{1,1}B)\xi + (c_{0,2}A + c_{1,2}B + c_{2,2}C)\xi^2$$

and

$$b(\xi) = A + B\xi + C\xi^2,$$

where

$$A = c_{1,3}c_{2,4} - c_{1,4}c_{2,3}, \qquad B = c_{2,3}c_{0,4} - c_{2,4}c_{0,3}, \qquad C = c_{0,3}c_{1,4} - c_{0,4}c_{1,3}.$$

Example 3. From Example 1, we have

$$\frac{g(\xi)}{h(\xi)} = \frac{-0.487492 - 0.231158\xi - 0.674078\xi^2}{0.455746 - 0.438713\xi + 0.514187\xi^2 + 0.942248\xi^3 + \xi^4}$$

and integration gives

$$\tfrac{1}{2}\theta(\xi) = 2\left[0.0125113 \ln\left|\frac{\xi + 0.830350 - 0.828652\mathrm{i}}{\xi - 0.359226 - 0.449591\mathrm{i}}\right| - 0.219377 \arg(\xi + 0.830350 - 0.828652\mathrm{i}) - 0.312214 \arg(\xi - 0.359226 - 0.449591\mathrm{i})\right] - 0.374956\pi.$$

Then we obtain the values

$f(0)$	$f'(0)$	$f(\frac{1}{2})$	$f(1)$	$f'(1)$
$+0.663502$	-1.54056	-0.112565	-0.663502	-0.810949

and the interpolant becomes

$$\frac{a(\xi)}{b(\xi)} = \frac{0.663502 - 1.37560\xi - 0.468837\xi^2}{1 + 0.248617\xi + 0.531233\xi^2}.$$

The error between the exact angle $\theta(\xi)$ and its approximation $\phi(\xi)$ is extremal at points where $\theta'(\xi) - \phi'(\xi) = 0$, which is equivalent to

$$\frac{g(\xi)}{h(\xi)} = \frac{a'(\xi)b(\xi) - a(\xi)b'(\xi)}{a^2(\xi) + b^2(\xi)}.$$

This is, in general, an algebraic equation of degree 6, which can be solved numerically to any desired accuracy. In this example, the roots on [0, 1] are

$$\xi = 0, \quad 0.273067, \quad 0.662032, \quad 1$$

(where 0 and 1 appear by virtue of the fact that $\phi(\xi)$ is, by construction, a C^1 Hermite interpolant to $\theta(\xi)$ at these points). The error attains its maximum magnitude 0.0136704 at $\xi = 0.273067$, corresponding to about 0.58% of the total variation of θ over the interval $\xi \in [0,1]$—in this case, $\theta(0) - \theta(1)$. The graphs of $\theta(\xi)$ and its approximant $\phi(\xi)$ are compared in Fig. 1—they are virtually indistinguishable. To emphasize the approximation error, Fig. 1 also compares the derivatives of these functions.

Example 4. From Example 2 we have

$$\frac{g(\xi)}{h(\xi)} = \frac{-0.563650 + 0.615068\xi - 0.615068\xi^2}{0.300523 + 0.324281\xi + 0.675719\xi^2 - 2\xi^3 + \xi^4}$$

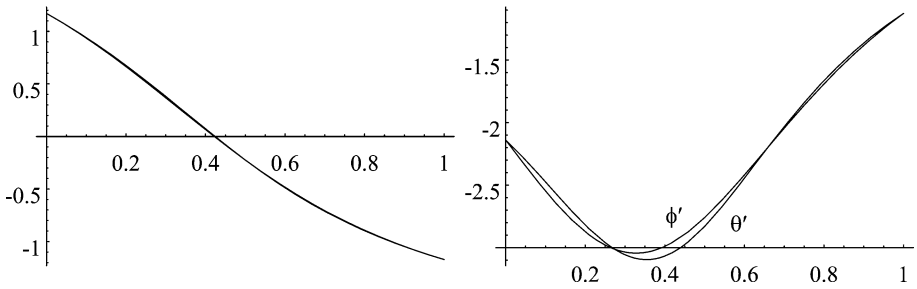

Fig. 1. Left: the exact angle function $\theta(\xi)$ and its approximation $\phi(\xi)$ in Example 3—the graphs are virtually indistinguishable at the scale shown. Right: comparison of the corresponding derivatives, $\theta'(\xi)$ and $\phi'(\xi)$.

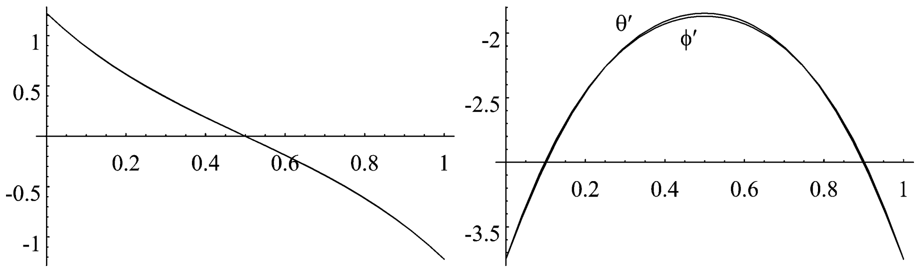

Fig. 2. Left: the exact angle function $\theta(\xi)$ and its approximation $\phi(\xi)$ in Example 4—again, the two graphs are virtually indistinguishable. Right: comparison of the corresponding derivatives, $\theta'(\xi)$ and $\phi'(\xi)$.

and integration yields

$$\tfrac{1}{2}\theta(\xi) = -2\cdot 0.431258\big[\arg(\xi+0.234351-0.356555\mathrm{i}) + \arg(\xi-1.23435-0.356555\mathrm{i})\big] + \theta_0.$$

Again, by choosing $\theta_0 = -0.862515\pi$, the argument of the tangent function lies in the interval $\pm 0.194414\pi$, and we have the values

$f(0)$	$f'(0)$	$f(\frac{1}{2})$	$f(1)$	$f'(1)$
$+0.700063$	-2.79476	0	-0.700063	-2.79476

for which the interpolant becomes

$$\frac{a(\xi)}{b(\xi)} = \frac{0.700063 - 1.40013\xi}{1 + 1.99215\xi - 1.99215\xi^2}.$$

In this case, the maximum error magnitude 0.00388068 is about 0.16% of the total variation of θ over $\xi \in [0,1]$, and occurs at $\xi = 0.250204$ and 0.749796. Fig. 2 compares $\theta(\xi)$ and $\phi(\xi)$, together with their derivatives, in this case.

Fig. 3 compares the variation of the Frenet frame, ERF, and rational approximation to the RMF, along the curve of Example 4. Compared to the rotation-minimizing frame, the “unnecessary” rotation of both the Frenet and Euler–Rodrigues frames is clearly apparent. The RMF is evidently a superior choice for use in applications such as animation, motion planning, and construction of swept surfaces.

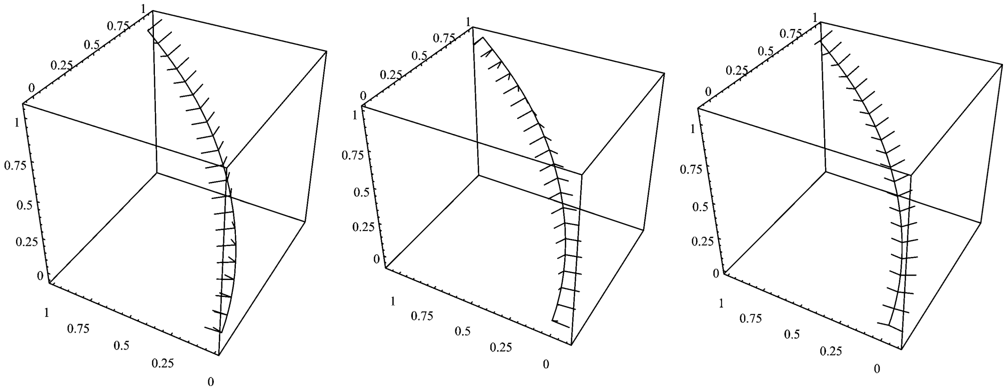

Fig. 3. Comparison of Frenet frame (left), Euler–Rodrigues frame (middle), and rational approximate rotation-minimizing frame (right) along the helical PH quintic of Example 4. For clarity, the tangent is omitted in each case. Rational approximation to the RMF clearly offers the most "reasonable" variation of a basis in the curve normal plane at each point.

Example 5. As a final example, consider a PH quintic Hermite interpolant to the end points $\mathbf{p}_i = (-1, 0, 0)$, $\mathbf{p}_f = (1, 0, 0)$ and derivatives $\mathbf{d}_i = \mathbf{d}_f = (1, 1, 0)$. Choosing parameters $\phi_0 = \phi_2 = -\pi/4$ and $\phi_1 = -\pi/2$ in the Hermite interpolation algorithm (Farouki et al., 2002b) yields the quaternion coefficients

$$\mathcal{A}_0 = \mathcal{A}_2 = 0.776887 + 0.776887\mathbf{i} + 0.321797\mathbf{j} + 0.321797\mathbf{k},$$
$$\mathcal{A}_1 = 2.54659 - 1.16533\mathbf{i} - 0.482696\mathbf{j} - 0.651072\mathbf{k}.$$

The remaining Bézier control points are then $\mathbf{p}_1 = -\mathbf{p}_4 = (-0.8, 0.2, 0.0)$ and $\mathbf{p}_2 = -\mathbf{p}_3 = (-0.512415, 0.112735, -0.265059)$. This example is constructed specifically to exhibit an inflection: the curvature vanishes at $\xi = 0.5$.

In this case, we have

$$\frac{g(\xi)}{h(\xi)} = \frac{5.65912 - 11.3182\xi}{1.41421 - 2.82390\xi + 36.8149\xi^2 - 67.9819\xi^3 + 33.9910\xi^4},$$

and integration gives

$$\tfrac{1}{2}\theta(\xi) = 2 \cdot 0.416848\big[\arg(\xi - 0.998568 + 0.200273\mathrm{i}) - \arg(\xi - 0.00143157 + 0.200273\mathrm{i})\big] - \frac{-0.496695}{\pi}.$$

The rational Hermite approximation to $f(\xi)$ is then

$$\frac{a(\xi)}{b(\xi)} = \frac{-0.448764 + 4.19880\xi - 4.19880\xi^2}{1 + 1.35636\xi - 1.35636\xi^2}.$$

Fig. 4 compares $\theta(\xi)$ with its approximation $\phi(\xi)$, and also their derivatives, while Fig. 5 shows (from left to right) the Frenet frame, ERF, and rational RMF approximation. Note that the Frenet frame "flips" upon passing through the inflection, at which point it is indeterminate.

The approximation scheme can achieve any prescribed accuracy by subdividing the $[0, 1]$ domain into sub-intervals, and constructing rational $(2, 2)$ approximants over those intervals. We have observed

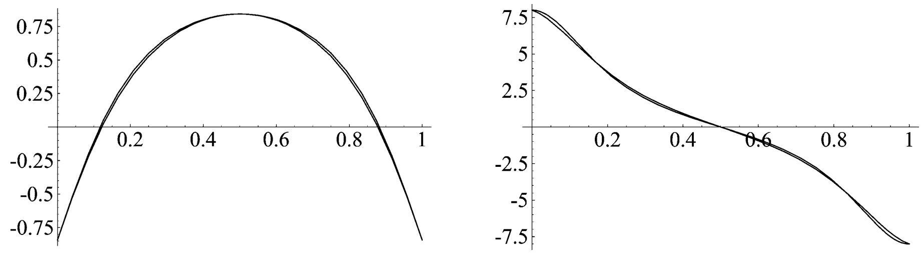

Fig. 4. Left: exact angle function $\theta(\xi)$ and its approximation $\phi(\xi)$ for Example 5. Right: the corresponding derivatives, $\theta'(\xi)$ and $\phi'(\xi)$.

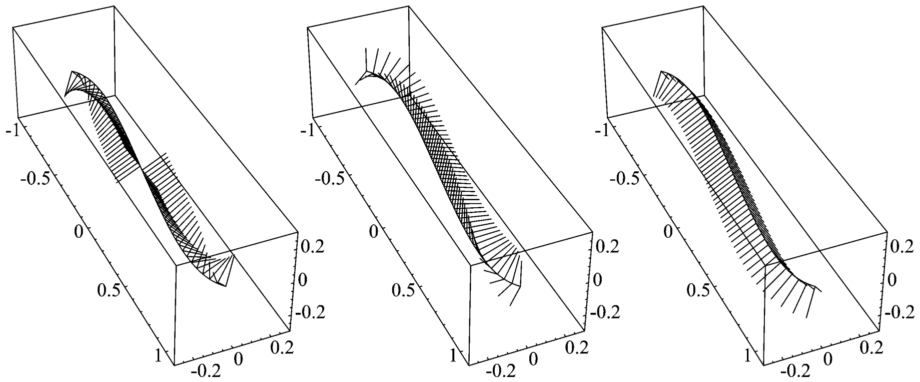

Fig. 5. Comparison of the Frenet frame (left), the Euler–Rodrigues frame (middle), and the rational approximate rotation-minimizing frame (right) on the PH quintic of Example 5 (for clarity, the tangent is omitted in each case). Note the sudden "flip" in the Frenet frame at the inflection point.

empirically that this approach often gives faster convergence to the exact RMF than higher-order rational approximants. Since the one-point Padé approximant of order (m,n) to a function $f(\xi)$ agrees with all terms in its Taylor series up to and including ξ^{m+n}, the approximant will have $\mathrm{O}(|\xi/R|^{m+n+1})$ error for $|\xi| < R$, where R is the radius of convergence[7] of the Taylor series (Baker and Graves-Morris, 1996). The convergence rates for multi-point Padé approximants or rational Hermite interpolants have not been investigated as thoroughly, but it seems likely that they are equivalent to those of one-point Padé approximants of the same order.

6. Closure

Adapted orthonormal frames are required in various applications involving three-dimensional motions along space curves. In order for an adapted frame to have a rational dependence upon the curve parameter, the curve must be a Pythagorean-hodograph (PH) curve. For most applications, the *rotation-minimizing frame* (RMF) is the most desirable among all possible adapted frames. Although PH curves admit exact

[7] Padé approximants may converge even outside the radius of convergence of the Taylor series—this fact is often used as a practical approach to analytic continuation.

derivations of the RMF, they incur transcendental functions. In this paper, a procedure to compute low-degree rational RMF approximations for PH curves has been presented. In typical cases, the scheme offers compact rational RMF approximations of excellent accuracy, that are well-suited to use in practical algorithms for computer-aided design, computer graphics, and visualization.

Acknowledgements

The first author was supported in part by the National Science Foundation, under grants CCR-9902669, CCR-0202179, and DMS-0138411. The second author was supported in part by KOSEF through the Statistical Research Center for Complex Systems at Seoul National University.

References

Baker, G.A., Graves-Morris, P., 1996. Padé Approximants, 2nd Edition. University Press, Cambridge.

Bangert, C., Prautzsch, H., 1997. Circle and sphere as rational splines. Neural Parallel Sci. Comput. 5, 153–161.

Bishop, R.L., 1975. There is more than one way to frame a curve. Amer. Math. Monthly 82, 246–251.

Brezinski, C., Van Iseghem, J., 1994. Padé approximations. In: Ciarlet, P.G., Lions, J.L. (Eds.), Handbook of Numerical Analysis III. Elsevier, Amsterdam, pp. 47–222.

Choi, H.I., Han, C.Y., 2002. Euler–Rodrigues frames on spatial Pythagorean-hodograph curves. Computer Aided Geometric Design 19, 603–620.

Choi, H.I., Lee, D.S., Moon, H.P., 2002. Clifford algebra, spin representation, and rational parameterization of curves and surfaces. Adv. Comp. Math. 17, 5–48.

Chou, J.J., 1995. Higher order Bézier circles. Computer-Aided Design 27, 303–309.

Cuyt, A., 1992. Rational Hermite interpolation in one and more variables. In: Singh, S.P. (Ed.), Approximation Theory, Spline Functions and Applications. Kluwer Academic, Dordrecht, pp. 69–103.

Dietz, R., Hoschek, J., Jüttler, B., 1993. An algebraic approach to curves and surfaces on the sphere and on other quadrics. Computer Aided Geometric Design 10, 211–229.

Dill, E.H., 1992. Kirchhoff theory of rods. Arch. Hist. Exact Sci. 44, 1–23.

Farouki, R.T., 1996. The elastic bending energy of Pythagorean hodograph curves. Computer Aided Geometric Design 13, 227–241.

Farouki, R.T., 2002. Exact rotation-minimizing frames for spatial Pythagorean-hodograph curves. Graph. Models 64, 382–395.

Farouki, R.T., Sakkalis, T., 1994. Pythagorean-hodograph space curves. Adv. Comp. Math. 2, 41–66.

Farouki, R.T., Shah, S., 1996. Real-time CNC interpolators for Pythagorean-hodograph curves. Computer Aided Geometric Design 13, 583–600.

Farouki, R.T., al-Kandari, M., Sakkalis, T., 2002a. Structural invariance of spatial Pythagorean hodographs. Computer Aided Geometry Design 19, 395–407.

Farouki, R.T., al-Kandari, M., Sakkalis, T., 2002b. Hermite interpolation by rotation-invariant spatial Pythagorean-hodograph curves. Adv. Comp. Math. 17, 369–383.

Farouki, R.T., Han, C.Y., Manni, C., Sestini, A., 2003. Characterization and construction of helical Pythagorean-hodograph quintic space curves. Preprint.

Farouki, R.T., Manjunathaiah, J., Nicholas, D., Yuan, G.-F., Jee, S., 1998. Variable feedrate CNC interpolators for constant material removal rates along Pythagorean-hodograph curves. Computer-Aided Design 30, 631–640.

Fiorot, J.-C., Jeannin, P., Cattiaux-Huillard, I., 1997. The circle as a smoothly joined BR-curve on $[0, 1]$. Computer Aided Geometric Design 14, 313–323.

Guggenheimer, H., 1989. Computing frames along a trajectory. Computer Aided Geometric Design 6, 77–78.

Jüttler, B., 1998. Generating rational frames of space curves via Hermite interpolation with Pythagorean hodograph cubic splines. In: Geometric Modeling and Processing ’98. Bookplus Press, pp. 83–106.

Jüttler, B., Mäurer, C., 1999a. Cubic Pythagorean hodograph spline curves and applications to sweep surface modelling. Computer-Aided Design 31, 73–83.

Jüttler, B., Mäurer, C., 1999b. Rational approximation of rotation minimizing frames using Pythagorean-hodograph cubics. J. Geom. Graphics 3, 141–159.

Klok, F., 1986. Two moving coordinate frames for sweeping along a 3D trajectory. Computer Aided Geometric Design 3, 217–229.

Kreyszig, E., 1959. Differential Geometry. University of Toronto Press, Toronto.

Landau, L.D., Lifshitz, E.M., 1986. Theory of Elasticity, 3rd Edition. Pergamon Press, Oxford.

Lembo, M., 2001. On the free shapes of elastic rods. Eur. J. Mech. A Solids 20, 469–483.

Love, A.E.H., 1944. A Treatise on the Mathematical Theory of Elasticity. Dover, New York (reprint).

Piegl, L., Tiller, W., 1989. A menagerie of rational B-spline circles. IEEE Comput. Graph. Appl. 9 (5), 48–56.

Steigmann, D.J., Faulkner, M.G., 1993. Variational theory for spatial rods. J. Elast. 33, 1–26.

Stoer, J., Bulirsch, R., 1992. Introduction to Numerical Analysis, 2nd Edition. Springer-Verlag, New York.

Struik, D.J., 1988. Lectures on Classical Differential Geometry. Dover Publications, New York (reprint).

Tsai, Y.-F., Farouki, R.T., Feldman, B., 2001. Performance analysis of CNC interpolators for time-dependent feedrates along PH curves. Computer Aided Geometric Design 18, 245–265.

Uspensky, J.V., 1948. Theory of Equations. McGraw-Hill, New York.

Wagner, M.G., Ravani, B., 1997. Curves with rational Frenet–Serret motion. Computer Aided Geometric Design 15, 79–101.

Wallner, J., Pottmann, H., 1997. Rational blending surfaces between quadrics. Computer Aided Geometric Design 14, 407–419.

Wang, W., Joe, B., 1997. Robust computation of the rotation minimizing frame for sweep surface modelling. Computer-Aided Design 29, 379–391.